MM-WAVE STANDING-WAVE ACCELERATING STRUCTURES FOR HIGH-GRADIENT TESTS *

E. A. Nanni†, M. dal Forno, V. A. Dolgashev, J. Neilson,
S. Tantawi, SLAC National Accelerator Laboratory, Menlo Park, USA
S. C. Schaub, R. J. Temkin, Massachusetts Institute of Technology, Cambridge, USA

Abstract

We present the design and parameters of single-cell accelerating structures for high-gradient testing at 110 GHz. The purpose of this work is to study the basic physics of ultrahigh vacuum RF breakdown in high-gradient RF accelerators. The accelerating structures consist of π-mode standing-wave cavities fed with the TM_{01} circular waveguide mode. The geometry and field shape of these accelerating structures is as close as practical to single-cell standing-wave X-band accelerating structures, more than 40 of which were tested at SLAC. This wealth of X-band data will serve as a baseline for these 110 GHz tests. The structures will be powered from a pulsed MW gyrotron oscillator. One MW of RF power from the gyrotron may allow us to reach a peak accelerating gradient of 400 MeV/m.

INTRODUCTION

Experimental data on the high-gradient performance of accelerating structures is an important aspect in deciding the operational frequency for an accelerator. RF breakdown is one of the major phenomena that limits the achievable gradient in accelerating structures. Extensive studies on RF breakdown in copper accelerating structures [1] have been performed at frequencies as high as X-band [2–6], Ku-Band [7] and Ka-Band [8–10]. Recently, we have expanded our experiments to the mm-wave range with beam-driven accelerators at FACET [11].

The statistical behavior of RF breakdown was observed during NLC/GLC work [2, 4, 12, 13], where after $10^5 - 10^7$ pulses at the same RF power and pulse shape, most accelerating structures approached a steady state or slowly decreasing RF breakdown rate. It is now common practice to measure and use the breakdown probability to quantify the performance of accelerating structures.

We propose to use a MW pulsed-power gyrotron oscillator at 110 GHz [14], originally developed for fusion plasma heating applications, for high gradient tests of mm-wave accelerators. We are aiming to achieve accelerating gradients well beyond 100 MeV/m and plan to measure RF breakdown statistics.

The RF parameters of accelerator cavities scale with frequency. This scaling can be obtained from the cavity geometry and its material properties. With increased frequency the shunt impedance increases ($\propto f^{1/2}$), and the energy required to achieve the desired accelerating gradient is reduced ($\propto 1/f^2$). Meanwhile, the surface resistivity increases with frequency ($R_s \propto f^{1/2}$). For the case of critically coupled cavities and a pulse length on the order of the fill time ($\sim 2\tau = 2Q_{\text{ext}}/\pi f \propto 1/f^{3/2}$), the pulsed heating decreases ($R_s \times \sqrt{2\tau} \propto 1/f^{1/4}$) for the same accelerating gradient.

ACCELERATING STRUCTURE SIMULATIONS

We consider standing-wave accelerating structures with cavity geometries that allow for direct comparison with experiments at 11.424 GHz conducted at the SLAC National Accelerator Laboratory [3]. The RF properties of the accelerating structures are primarily determined by the a/λ ratio for the structure where a is the radius of the iris aperture and λ is the operational wavelength. An example of the geometry, field distribution and dimensions for one of the periodic accelerating cavities at 110 GHz ($a/\lambda = 0.215$) is shown in Fig. 1.

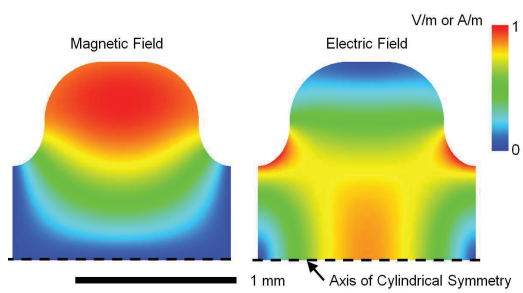

Figure 1: Normalized magnetic and electric field distribution for the TM_{01} π-mode of the A0.586-T0.4-Cu accelerating cavity. For 100 MeV/m accelerating gradient the peak surface electric field is 225 MV/m and the the peak surface magnetic field is 0.391 MA/m.

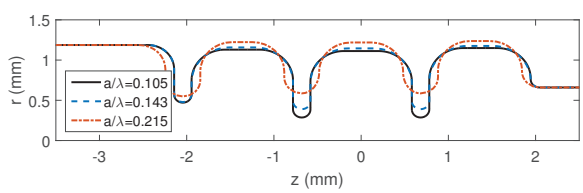

Figure 2: The cavity profile for the standing-wave accelerating structures.

Ideally, a 1:1 scaling of cavity geometry from 11.424 GHz to 110 GHz is desired to understand how

* This work was supported by Department of Energy contract DE-AC02-76SF00515.
† nanni@slac.stanford.edu

Table 1: π-mode, 110 GHz periodic cavity parameters with a cell length of 1.36 mm. Fields are normalized for E_{acc} = 100 MeV/m accelerating gradient

Name	Unit	A0.286-T0.2-Cu	A0.390-T0.2-Cu	A0.586-T0.4-Cu
Stored Energy	[μJ]	173	217	336
Q_0	[x1000]	3.17	3.26	3.16
Shunt Impedance	[MΩ/m]	362	297	185
Max. Surface Mag. Field, H_{max}	[MA/m]	0.276	0.300	0.391
Max. Surface Elec. Field, E_{max}	[MV/m]	227	229	225
$K_e = E_{max}/E_{acc}$		2.27	2.29	2.25
Losses in One Cell	[kW]	37.6	46.0	73.5
Iris Aperture Radius, a	[mm]	0.286	0.390	0.586
a/λ		0.105	0.143	0.215
$H_{max} Z_0/E_{acc}$		1.04	1.13	1.47
Iris Thickness, t	[mm]	0.2	0.2	0.4
Iris Ellipticity		1	1.35	1.3

Table 2: Single-cell π-mode cavity parameters. Fields are normalized to 1 MW of dissipated power. Accelerating gradient is defined as the peak surface electric field divided by K_e.

Name	Unit	A0.286-T0.2-Cu	A0.390-T0.2-Cu	A0.586-T0.4-Cu
Max. Surface Elec. Field, E_{max}	[MV/m]	916	827	624
Max. Surface Mag. Field, H_{max}	[MA/m]	1.13	1.13	1.16
Accelerating Gradient	[MeV/m]	404	361	277
Max. Surface Poynting Vector, S	[W/(μm)^2]	549	590	539
S/H_{max}^2	[Ω]	430	462	401
Peak Pulsed Heating (20 ns Square Input Pulse)	[^{o}C]	156	156	165

the RF performance changes with frequency. Accelerating cavities with a/λ ratios of 0.105, 0.143 and 0.215 were extensively studied at X-band [3]. However, practical considerations related to the ability to manufacture these structures does not allow for identical geometries scaled from 11.424 GHz to 110 GHz. Therefore, we increased the ratio of iris thickness t to λ. We will compare performance of 11.424 GHz and 110 GHz cavities by considering the surface electric and magnetic fields, pulsed heating and peak surface Poynting vector.

In Table 1 we list the RF parameters for the single-cell structures with periodic master/slave boundary conditions simulated in HFSS [15]. The outer diameter radius of curvature was increased for the mm-wave structures to allow for fabrication. This increased radius reduced the ratio of the peak surface magnetic field to accelerating gradient. We designed the iris shape to maintain a similar peak surface electric field to accelerating gradient ratio ($\sim$ 2.25) for all three cavities.

The periodic structures were used to create single-cell standing-wave accelerating cavities for our breakdown tests. This cavity has three cells, but we made the field in the central cell twice as high as in the adjacent cells. This was done to ensure that most of the breakdowns are in the central cell with boundary conditions that mimic a standing wave structure with many cavities. The accelerating structure is axially coupled through a 1.187 mm radius cylindrical waveguide operating in the TM_{01} mode. On the other side of the structure there is a 0.660 mm radius beam pipe below cutoff for the TM_{01} mode. The cavity profile for the three structures is shown in Fig. 2. The boundary conditions for the outer wall are copper.

The RF parameters of the structures is given in Table 2. The fields were normalized for 1 MW of dissipated power with which we expect to test them. The electric field, magnetic field and Poynting vector along the contour of the metallic surface plotted in Fig. 2 are shown in Fig. 3. The electric field on-axis is shown in Fig. 4. Note that for the same dissipated power the structures have similar peak surface magnetic fields, but the peak surface electric field and thus the accelerating gradient (given by Table 2) vary by $\sim$ 50%.

An important parameter to consider is the peak pulsed heating of the metal surface [16]. In our structures with 1 MW of dissipated power and a 20 ns square pulse from the source ($\sim 2\tau = 20\ ns$), this pulsed heating exceeds 150^{o}C in all three structures, see Table 2. The maximum surface temperature vs time for A0.390-T0.2-Cu is shown in Fig. 5.

ISBN 978-3-95450-147-2

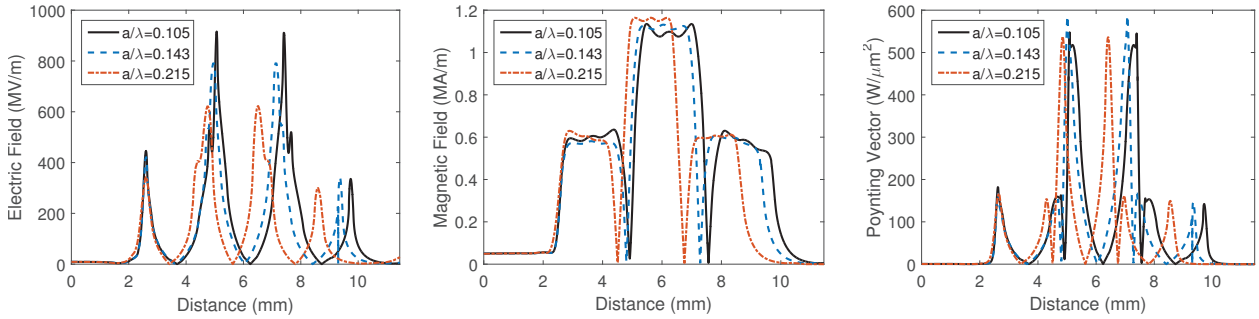

Figure 3: The (a) electric field, (b) magnetic field and (c) Poynting vecor for all three standing-wave accelerating structures on the metallic surface shown in Fig. 2 for 1 MW of dissipated power in the structure.

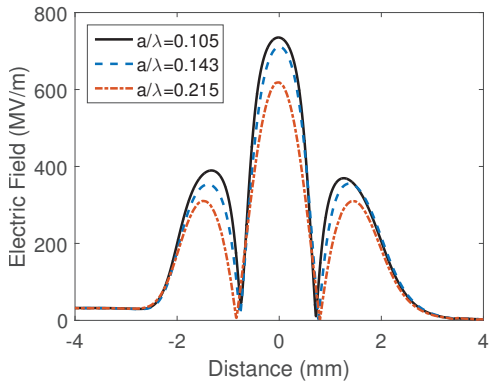

Figure 4: The electric field on-axis for the cavities shown in Fig. 2 for 1 MW of dissipated power in the structure.

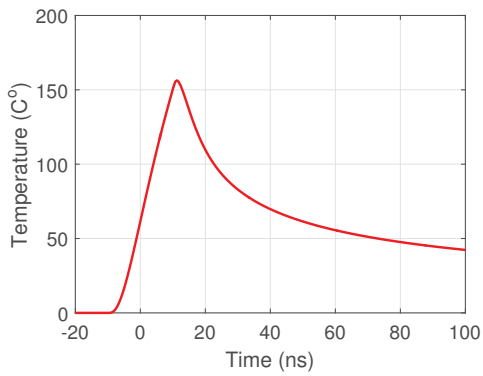

Figure 5: Maximum surface temperature for A0.390-T0.2-Cu as a function of time when the cavity is driven by a 20 ns, 1 MW square pulse.

FULL RF STRUCTURE

We plan to use a 1 MW 110 GHz gyrotron to power our accelerating structures. The gyrotron power is transported in a free-space Gaussian mode. In order to couple into the accelerating structure we convert the Gaussian beam into the TM_{01} mode of a circular waveguide. The profile of the mode converter is shown in Fig. 6. First, the Gaussian beam will be focused onto the aperture of a smooth-walled horn with ~6 mm beam waist. The horn converts the Gaussian beam into the TE_{11} mode with ~99% conversion efficiency and is tolerant to miss-alignments and offsets with a reduction of only 5% in power coupling efficiency for a $\pm 2^o$ tilt or ±1 mm offset. Following the Gaussian converter is a TE_{11} to TM_{01} mode converter, which includes a 90 degree bend. The mode converter has a 97% power conversion efficiency and a bandwidth exceeding 2 GHz. This bandwidth is larger than the tunable frequency range of the gyrotron oscillator.

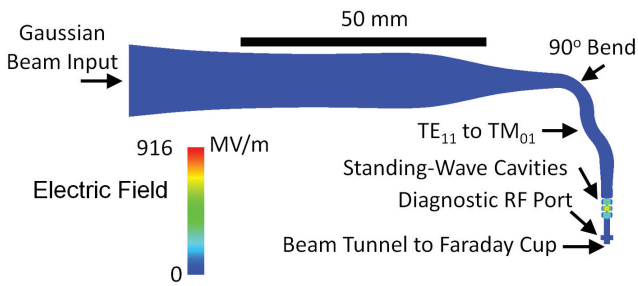

Figure 6: Electric field distribution on the symmetry plane of the assembly consisting of the mode converter and the standing-wave accelerating structure A0.286-T0.2-Cu. Fields are shown for 1 MW in the Gaussian beam.

CONCLUSION

We have presented the design and parameters of single-cell accelerating structures for high-gradient testing at 110 GHz. The RF design including the performance of the mode converters may allow us to reach peak accelerating gradients of 400 MeV/m with 1 MW of RF power from a 110 GHz gyrotron oscillator.

ACKNOWLEDGMENT

The authors thank Michael Shapiro, Andy Haase and Gordon Bowden for helpful discussions.

REFERENCES

[1] Chang, Chao, et al., "Review of recent theories and experiments for improving high-power microwave window breakdown thresholds", *Physics of Plasmas*, 18.5 (2011): 055702.

[2] Döbert, Steffen, et al., "High gradient performance of NLC/GLC X-band accelerating structures", in *Proc. of IPAC 2005*, Knoxville, Tennessee, 2005, pp. 372-374.

[3] Dolgashev, Valery, et al., "Geometric dependence of radio-frequency breakdown in normal conducting accelerating structures", *Applied Physics Letters*, 97.17 (2010): 171501.

[4] Higo, Toshiyasu, et al., "Advances in X-band TW Accelerator Structures Operating in the 100 MV/m Regime", in *Proc. of IPAC 2010*, Kyoto, Japan, THPEA013, (2010), p. 3702.

[5] Marsh, Roark A., et al., "X-band photonic band-gap accelerator structure breakdown experiment", *Physical Review Special Topics-Accelerators and Beams*, 14.2 (2011): 021301.

[6] Degiovanni, A., et al., "High-Gradient Test Results From a CLIC Prototype Accelerating Structure: TD26CC", in *Proc. of IPAC2014*, Dresden, Germany, WEPME015. 2014.

[7] Munroe, Brian J., et al., "Experimental high gradient testing of a 17.1 GHz photonic band-gap accelerator structure", *Physical Review Accelerators and Beams* 19.3 (2016): 031301.

[8] Achard, C., et al., "30 GHz power production in CTF3", in *Proc. of IPAC 2005*, Knoxville, Tennessee, 2005, pp. 1695-1697.

[9] Rodriguez, J., et al., "30 GHz high-gradient accelerating structure test results", in *Proc. of PAC07*. Albuquerque, New Mexico, FROBC01, 2007.

[10] Grudiev, Alexej, S. Calatroni, and W. Wuensch, "New local field quantity describing the high gradient limit of accelerating structures", *Physical Review Special Topics-Accelerators and Beams* 12.10 (2009): 102001.

[11] Dal Forno, Massimo, et al., "rf breakdown tests of mm-wave metallic accelerating structures", *Physical Review Accelerators and Beams* 19.1 (2016): 011301.

[12] J. W. Wang, "R&D of accelerator structures at SLAC", *High Energy Phys. Nucl. Phys.* 30, 11 (2006).

[13] C. Adolphsen, "Normal Conducting rf Structure Test Facilities and Results", in *Proceedings of the 2003 Particle Accelerator Conference*, Portland, OR (IEEE, New York,2003), p. 668.

[14] Tax, David S., et al. "Experimental Results for a Pulsed 110/124.5-GHz Megawatt Gyrotron", *Plasma Science, IEEE Transactions on* 42.5 (2014): 1128-1134.

[15] ANSYS Electronics Desktop 16.2, *HFSS*.

[16] Pritzkau, David P., and Robert H. Siemann, "Experimental study of RF pulsed heating on oxygen free electronic copper", *Physical Review Special Topics-Accelerators and Beams* 5.11 (2002): 112002.

ISBN 978-3-95450-147-2